Mathematical Modelling of the Effects of Plasma Treatment on the Diffusivity of Biofilm

Tripti Thapa Gupta [1] , **Surya B. Karki** [1], **Ronald Fournier** [1] and **Halim Ayan** [1,2,*]

[1] Department of Bioengineering, College of Engineering, University of Toledo, Toledo, OH 43606, USA; tripti.thapa@rockets.utoledo.edu (T.T.G.); surya.karki@rockets.utoledo.edu (S.B.K.); Ronald.fournier@utoledo.edu (R.F.)

[2] Department of Mechanical, Industrial and Manufacturing Engineering, College of Engineering, University of Toledo, Toledo, OH 43606, USA

[*] Correspondence: halim.ayan@utoledo.edu; Tel.: +1-419-530-8126

check for
updates

Abstract: Biofilm formation on implanted medical devices is the reason for most of the nosocomial infections in clinical settings. Biofilms are more resistant to antimicrobials than their planktonic cells mainly because of the presence of the matrix of extracellular polymeric substances (EPSs), which acts as a physical barrier that limits the transport of antimicrobials inside the biofilm. A combinatorial antimicrobial approach of a non-thermal plasma and chlorhexidine (CHX) digluconate can be used to sterilize those surfaces contaminated with biofilm. However, the reason behind achieving this combinatorial decontamination is not known. Thus, in this study, we developed a mathematical model to explain the reason behind sterilization with the combinatorial treatment approach. It was found that the application of plasma prior to treatment with CHX is disrupting the biofilm and making it very porous. This is allowing CHX to penetrate deeper inside the porous biofilm, which is then effective at sterilizing the biofilm.

Keywords: biofilm; Pseudomonas aeruginosa; non-thermal plasma; CHX; diffusion; mathematical modelling

1. Introduction

The biofilm is one of the most prevalent types of growth in nature and is critical in the development of various clinical infections [1]. Biofilms develop when microorganisms come together and adhere to surfaces. These surfaces may be drinking water pipes, indwelling medical devices, or a human tissue [2]. The microorganisms within the biofilm are protected by a matrix formed by the bacteria known as extracellular polymeric substances (EPSs), which consists of polysaccharides, proteins, and extracellular DNA (eDNA). EPS maintains the structural integrity of the biofilm, allowing the bacteria to adapt to the surrounding environment [3]. Moreover, the EPS bind cells to the surface and to one another, which blocks the diffusion of antimicrobials to the microcolonies that are forming and protecting the biofilm from the host's defense mechanism [2]. The EPS preventing the diffusion of antimicrobials and from the host's defense mechanism are responsible for various infections in the clinical setting. Whenever a biofilm develops on implanted medical devices such as catheters and orthopedic implants, it becomes hard to eradicate them by chemotherapeutic and other sterilization processes [4]. Thus, biofilm associated infections such as catheter-related blood stream infections and prosthetic joint infections become problematic and difficult to control [4]. Removal of the medical device or internal prosthesis will be the primary surgical treatment for such chronic infections associated with the biofilm. Even with surgical treatment, there are several disadvantages such as increased patient morbidity and mortality, higher health care costs because of repeated surgeries,

extended hospitalization, rehabilitation, and antibiotic therapy [5]. Therefore, new alternatives such as non-thermal plasma for clinical infections treatment are critical to study. There has recently been a few studies using nonthermal plasma source for endoscopic plasma delivery [6,7]. One of the study published by Robert et al. demonstrated the development of a unique pulsed plasma gun for several applications such as remote high voltage fast commutation, plasma medicine applications, and small diameter catheters decontamination [8]. Such a plasma gun produced very fast-moving plasma bullets of nanosecond duration or bullet bursts from a pulsed dielectric barrier discharge (DBD) reactor. These kind of plasma can be propagated inside branched complex organs and plasma across needles or catheters that open up new opportunities for plasma technology in clinical applications and medical device disinfection [6].

Use of non-thermal plasma in combination with chlorhexidine (CHX) could conceivably be a suitable antimicrobial tool for removing these biofilms in clinical settings. The biocide CHX is one of the most widely used antiseptics for decontaminating skin, oral, and medical devices. Plasma is mainly a cocktail of positively and negatively charged ions, electrons, neutral atoms, molecules, and electric field [9–12], and is used extensively for bacterial sterilization and decontamination [13,14], cancer treatment [15,16], wound healing and disinfection [17,18], and in vitro blood coagulation [19]. One of the reviews published by Ehlbeck et al. discusses an overview of atmospheric pressure plasma sources (APPS) for microbial decontamination [20]. Various plasma sources such as corona discharges, dielectric barrier discharge (DBD), atmospheric pressure plasma jet, and microwave driven discharges are used for microorganism decontamination, as discussed in the cited review article. In a study done by Scholtz et al., complete inactivation of bacteria in liquid within 5 min was achieved by DC corona plasma exposure in ambient air [21]. Another DBD plasma source used by Fridman et al. resulted in complete inactivation of 10^7 and 10^8 CFU (colony forming unit) within 10 and 15 s of plasma treatment [19]. Ehlbeck et al. implemented atmospheric pressure plasma jet for catheter contaminated with a suspension of *Staphylococcus aureus* bacteria and reveals 5 and 6 log (complete inactivation) reduction for pure argon and with argon mixed with 0.25% air, respectively [22]. Another study by Sato et al. demonstrates complete inactivation of *E. coli* after 600 s of conventional atmospheric pressure microwave plasma source usage [23]. Similarly, Belgacem et al. developed a non-thermal plasma discharge inside a sealed bag which showed a 6 log reduction of *P. aeruginosa* and *S. aureus* in 45 and 120 min, respectively, and 4 log reduction of *B. subtilis* spores in 120 min [24]. One of the studies done with biofilm demonstrated nearly 100% of biofilm inactivation after 5 min of gas discharge plasma treatment [25]. Plasma has also been used effectively in dentistry. The dentin discs with *E. Faecalis* biofilm treated with plasma for 5 min resulted in 92.4% killing of cells, which has a potential to replace existing treatment for root canal disinfection [26]. Thus, the various active plasma agents such as NO, atomic oxygen (O), ozone (O_3), hydroxyl (OH), reactive oxygen (ROS) and nitrogen species (RNS), and high energy UV radiation are what makes these plasma an effective antimicrobial tool in several biomedical applications [20]. Electric field (EF) is another plasma agent that might be used for several biomedical applications and has been studied recently [12]. Robert et al. experimentally measured the EF that reveals the propagation of plasma in region of an intense longitudinal EF component [11]. The authors further speculate that the plasma treatment could be a unique way to deliver intense transient EF and chemical reactive species. Another study by Bourdon et al. showed the EF measurement within the plasma plume and mentions its importance for interactions to the plasma plume with surfaces in biomedical applications [10]. Similarly, several investigations have been made to identify the role of single plasma agents for the microorganism inactivation process [20]. The study carried by Dobrynin et al. states that both positive and negative plasma ions plays an important role in the interaction between biological organisms and plasma [20]. There are different mechanisms to inactivate microorganisms involving neutral, ionized and reactive species, and UV photons [24]. Initially, the fastest decrease in bacterial concentration is dominated by the UV radiations. These UV radiations damage the bacterial cell wall and penetrate the cell, which then inhibits the bacterial replication by damaging DNA. Similarly, charged particles and RONS (reactive oxygen and nitrogen

species) initiate the bacterial membrane alteration by photodesorption or etching mechanisms [24]. The study by Machala et al. [27] states that in atmospheric pressure plasma, the major decontaminating factors are radicals, ROS (e.g., OH, O, O_3) charged particles (O_2^-), which causes oxidative damage to different cellular components [28]. UV radiation plays a role if photons in UV C germicide region or in vacuum UV are produced. Another study also states that the synergic action of reactive and/or charged particles plays a major role for cell wall damage, with UV radiation playing only a minor role [29].

The two principal theories used to explain the biofilm being more resistant to the antimicrobial treatment are based on transport limitations and its ability to protect the bacterial cells within the biofilm [30]. Transport-based explains biofilm resistance acting as a barrier to antibiotic diffusion. Bacterial protection is the result of the reduced susceptibility of bacteria in biofilm compared with the bacteria in planktonic phase [30]. Inactivation of the antimicrobial treatment by the matrix EPS and the inability of the antimicrobial molecules to diffuse through these EPS matrix are the primary reasons for biofilm resistant to the antimicrobial treatment [2]. There are some previous works explaining the antimicrobial resistance of the biofilm caused by diffusion limitations. Suci et al. investigated the Ciprofloxacin penetration into *pseudomonas aeruginosa* biofilms. They found that the transport of the antibiotic to the biofilm-substratum interface was found to be impeded by the biofilm [31]. Hoyle et al. reported that the tobramycin diffusion across biofilms was the reason for dispersal of cells from the biofilm [2]. Nichols et al. hypothesized that polysaccharides played a major role in antibiotic diffusion, so they developed a physical model of microcolonies and biofilms to predict antibiotic penetration times. The authors also described diffusion of antibiotics into aggregates of *P. aeruginosa* [32]. These dispersed cells were more susceptible to tobramycin than the cells present within the biofilm. These studies were based on studying th-e reason behind antimicrobial resistance in biofilm in terms of diffusion. However, no studies have been done to investigate the reason for better penetration of biocide such as CHX after non-thermal plasma treatment of a biofilm. This study explains how the diffusion of CHX is enhanced after the plasma treatment in *P. aeruginosa* biofilm with mathematical modeling. A mathematical model of CHX diffusion was developed to explain the enhanced killing of *P. aeruginosa* biofilm after plasma treatment. This model further reports the impact of plasma treatment in combination with the biocide CHX for biofilm removal and can be assessed in future experimental work. Moreover, this model will provide knowledge on plasma decontamination and sterilization for challenging biomedical applications.

2. Materials and Methods

2.1. Development of a Mathematical Model of CHX Diffusion in a Biofilm

The mathematical development of CHX diffusion in a biofilm is based on Crank (1975) and Fournier (2017) [33]. The Figure 1 shows the physical characteristics of the biofilm. In this figure, S is the surface area of the biofilm normal to the CHX diffusion and δ is the thickness of the biofilm.
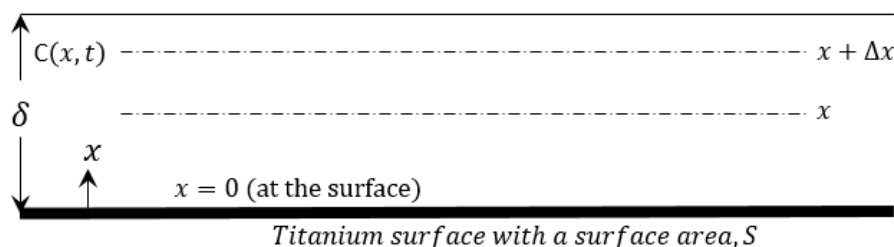

Figure 1. Biofilm model on a titanium surface.

Considering a thin slice in the biofilm (from x to $x + \Delta x$), the accumulation of CHX at time t is given by $S\Delta x \frac{\partial C}{\partial t}$. Now, from the mass-balance equation, *accumulation = in − out + generation − consumption*, and using Fick's law to describe CHX diffusion we obtain,

$$S\Delta x \frac{\partial C}{\partial t} = D_e S \frac{\partial C}{\partial x}\Big|_{(x+\Delta x)} - D_e S \frac{\partial C}{\partial x}\Big|_{(x)} \tag{1}$$

where D_e is the effective diffusivity of CHX in the biofilm and C is the biofilm concentration of CHX. It should be noted that in Equation (1), CHX generation is zero and CHX consumption is zero, because CHX degradation is assumed to be negligible during the treatment time as CHX is known to be a very stable molecule. The lifetime of CHX is in the order of days and even weeks [34,35]. Equation (1) then becomes,

$$\frac{\partial C}{\partial t} = D_e \frac{\partial^2 C}{\partial x^2} \tag{2}$$

The initial and boundary conditions for Equation (2) are,

$$
\begin{aligned}
&\text{Initial condition; } t = 0, \ C = 0 \\
&\text{Boundary condition 1 : at } x = 0, \ \tfrac{\partial C}{\partial x} = 0 \\
&\text{Boundary condition 2 : at } x = \delta, \ C = C_b
\end{aligned}
\tag{3}
$$

where C_b is the bulk concentration of the CHX.

From Crank (1975), the solution to Equations (2) and (3) is given by,

$$C(x,t) = c_b \left[1 - \frac{4}{\pi} \sum_{n=0}^{\infty} \frac{(-1)^n}{2n+1} \cdot \exp\left[\frac{-D_e(2n+1)^2 \pi^2 t}{4\delta^2} \right] \cdot \cos\left[\frac{(2n+1)\ \pi\ x}{2\delta} \right] \right] \tag{4}$$

From the definition of effective diffusivity,

$$D_e = \frac{\varepsilon D_{AB}}{\tau} \tag{5}$$

where D_{AB} is the diffusivity of CHX in the media assumed to have the same properties as water, τ is the tortuosity, and ε is the porosity.

From Fournier 2017, and using the molecular weight (MW) of CHX as 505 g/mole, we can estimate D_{AB} in water at 37 °C,

$$
\begin{aligned}
D_{AB} &= 1.013 \times 10^{-4} (MW)^{-0.46} \\
&= 5.782 \times 10^{-6} \, \text{cm}^2/\text{s}
\end{aligned}
$$

We can then adjust this value of D_{AB} at 20 °C using the Stokes–Einstein equation (Fournier 2017),

$$
\begin{aligned}
D_{AB} &= 5.782 \times 10^{-6} \times \tfrac{293}{310} \times \tfrac{0.691}{1.002} \\
&= 3.77 \times 10^{-6} \ \text{cm}^2/\text{s}
\end{aligned}
$$

where 0.691 and 1.002 are the viscosities of water at 310 K and 293 K, respectively.

Now consider the cell balance within the biofilm, we let

$$\overline{X} = \frac{Number\ of\ cells}{Volume\ of\ biofilm} \tag{6}$$

where $\overline{X}$ is the cell concentration based on the total film volume assuming that the cells remain stationary, that is, the cells do not move or diffuse. The death rate of the cells in the biofilm is proportional to the total amount of cells. The proportionality constant is the specific death rate (μ_d),

$$\frac{d\overline{X}}{dt} = \mu_d \, \overline{X} \quad \text{and,} \, \mu_d = k_d \, C(x,t) \tag{7}$$

The specific death rate constant, μ_d is assumed to depend on the local concentration of CHX, which is given by Equation (4), and a death rate constant k_d. Equation (7) then becomes,

$$\frac{d \ln \overline{X}}{dt} = -k_d C(x,t) \tag{8}$$

Integrating Equation (8) from the initial cell concentration $(\ln \overline{X}_0)$ at $t = 0$ to a final cell concentration $(\ln \overline{X})$ at time t.x

$$\overline{X}(x,t) = \overline{X}_0 e^{-k_d \int_0^t C(x,t)dt} \tag{9}$$

Equation (9) shows how the cell concentration at any given position or value of x changes with time. Now, let ϕ = total number of cells in the biofilm at time t. Then, the total number of cells measured in the biofilm at time t is given by,

$$\phi(t) = S \int_0^\delta \overline{X}(x,t)dx \tag{10}$$

At $t = 0$, the initial number of cell concentration is $\phi_0 = \overline{X}_0 \, S \, \delta$.

$$\frac{\phi_0}{\delta} = \overline{X}_0 \, S \tag{11}$$

Therefore, inserting Equation (9) into (10),

$$\phi(t) = S \, \overline{X}_0 \int_0^\delta e^{-k_d \int_0^t C(x,t)dt} dx \tag{12}$$

From Equations (11) and (12),

$$\frac{\phi(t)}{\phi_0} = \frac{1}{\delta} \int_0^\delta e^{-k_d f(x,t)} dx \tag{13}$$

where

$$f(x,t) = \int_0^t C(x,t)dt \tag{14}$$

Substituting the value of $C(x,t)$ from Equation (4) into (14) and interchanging, we get $f(x,t)$ as,

$$f(x,t) = C_b \left\{ t - \frac{16\delta^2}{\pi^3 D_e} \sum_{n=0}^\infty \frac{(-1)^n}{(2n+1)^3} \cdot \left[1 - exp\left[\frac{-D_e(2n+1)^2\pi^2 t}{4\delta^2} \right] \right] \cos\left[\frac{(2n+1)\pi x}{2\delta} \right] \right\} \tag{15}$$

As Equation (15) is very complex and we expect the summation to converge rapidly as t increases, we only use the term for $n = 0$. Therefore,

$$f(x,t)|_{n=0} = C_b \left\{ t - \frac{16\delta^2}{\pi^3 D_e} \cdot \left[1 - \exp\left[\frac{-D_e \pi^2 t}{4\delta^2} \right] \right] \cdot \cos\left[\frac{\pi x}{2\delta} \right] \right\} \tag{16}$$

For steady state (SS) or long treatment times,

$$f(x,SS)|_{n=0} = C_b \left[t - \frac{16\delta^2}{\pi^3 D_e} \cos\frac{\pi x}{2\delta} \right] \tag{17}$$

and at $x = 0$ (at the coupon surface),

$$f(0, SS)|_{n=0} = C_b \left[t - \frac{16\delta^2}{\pi^3 D_e} \right] \tag{18}$$

Further, at $x = \delta$,

$$f(\delta, SS)|_{n=0} = C_b \, t \tag{19}$$

Now, because the biofilm is very thin, we use the average value of the function f across the biofilm, which can be written as,

$$\overline{f}(t)|_{n=0} = \frac{1}{\delta} \int_0^\delta f(x, t)|_{n=0} dx \tag{20}$$

From Equations (16) and (20), we obtain,

$$\overline{f}(t)|_{n=0} = C_b \left[t - \frac{32\delta^2}{\pi^4 D_e} \cdot \left[1 - \exp\left[\frac{-D_e \pi^2 t}{4\delta^2} \right] \right] \right] \tag{21}$$

Substituting the result into Equation (13), we obtain,

$$\frac{\phi(t)}{\phi_0} = \frac{1}{\delta} \int_0^\delta e^{-k_d \overline{f}(t)|_{n=0}} dx = e^{-k_d \overline{f}(t)|_{n=0}} \tag{22}$$

From Equation (21), for $t > \tau = \frac{4\delta^2}{\pi^4 D_e}$, Equation (21) becomes,

$$\overline{f}(t)|_{n=0} = C_b \left(t - \frac{32\delta^2}{\pi^4 D_e} \right) \tag{23}$$

Then, using this result in Equation (22),

$$\frac{\phi(t)}{\phi_0} = e^{-k_d \overline{f}(t)|_{n=0}} = e^{-k_d C_b (t - t_{lag})} \tag{24}$$

where ϕ is the final number of cells after plasma treatment; ϕ_0 is the initial number of cells before plasma treatment; and t_{lag} is the x-intercept of the linear plot of $log_{10} \frac{\phi}{\phi_0}$ versus CHX treatment time, which is given by the equation,

$$t_{lag} = \frac{32\delta^2}{\pi^4 D_e} \tag{25}$$

Now, taking the log of Equation (24), we get,

$$log_{10} \frac{\phi(t)}{\phi_0} = \frac{k_d C_b}{2.303} t_{lag} - \frac{k_d C_b}{2.303} t \tag{26}$$

Equation (26) says a plot of $log_{10} \frac{\phi}{\phi_0}$ versus t should be linear. The value of t_{lag} can be found at that time where the regression line crosses the time axis. From the calculated t_{lag}, we can then find the effective diffusivity of CHX in the biofilm from Equation (25). The calculated value of D_e should be less than the previously calculated value of the effective diffusivity of CHX in water at 20 °C ($D_e = 3.77 \times 10^{-6} \mathrm{cm}^2 / \mathrm{sec}$). From the value of D_e, we can estimate the biofilm porosity, which will give us an idea on the extent of biofilm disruption by the plasma treatment.

2.2. Jet Plasma Generation and Electrical and Optical Characterization

A schematic diagram and a photograph of the jet plasma used in this study are shown in Figure 2. The details on the experimental and operating conditions of the jet plasma are given in the study [5,36] that we published earlier. The jet plasma operates at 1 kHz frequency with 10 kV. The gases used were 100% helium (He) at a total flow rate of 1 standard liters per minute (SLPM) into ambient air.

Figure 2. Schematic diagram and photograph of the jet plasma setup. The figure on the left demonstrates the schematic diagram of the jet plasma and the photograph on the right shows the actual experimental setup of jet plasma treating the Ti coupon (12.7 mm diameter and 3 mm thickness).

For electrical characterization as described in detail in the previous study [5], the changes in voltage and current waveforms of the jet plasma system were analyzed using a digital oscilloscope (Figure 3). These are the typical electrical waveforms that is generated by non-thermal plasma.
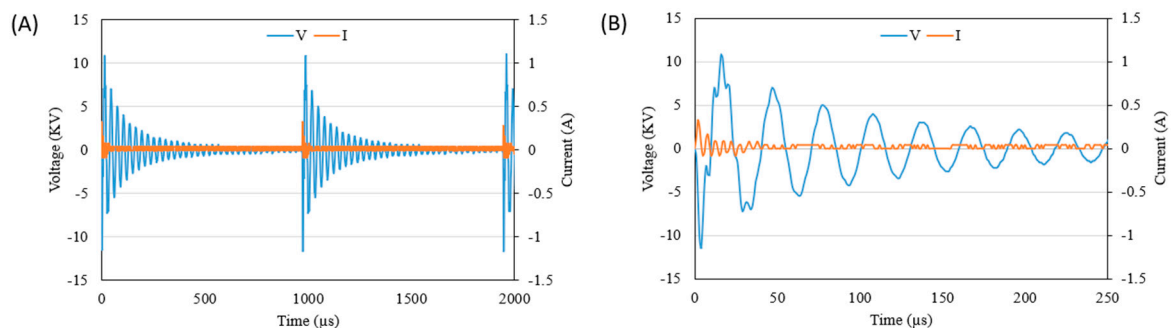

Figure 3. (**A**) Voltage and current waveforms of jet plasma. Two complete cycles based on 1 kHz frequency and 4 µs pulse width are shown; (**B**) A close-up view of the voltage and the current waveforms.

The optical characterization of jet plasma combined with He gas was characterized using optical emission spectroscopy (OES) to detect the reactive species generated in the plasma as shown in Figure 4. The details can be found in the previous study [5]. Various plasma species such as OH molecular spectrum, N_2 Molecular spectrum, excited atom emission lines, and NO and He lines were observed.
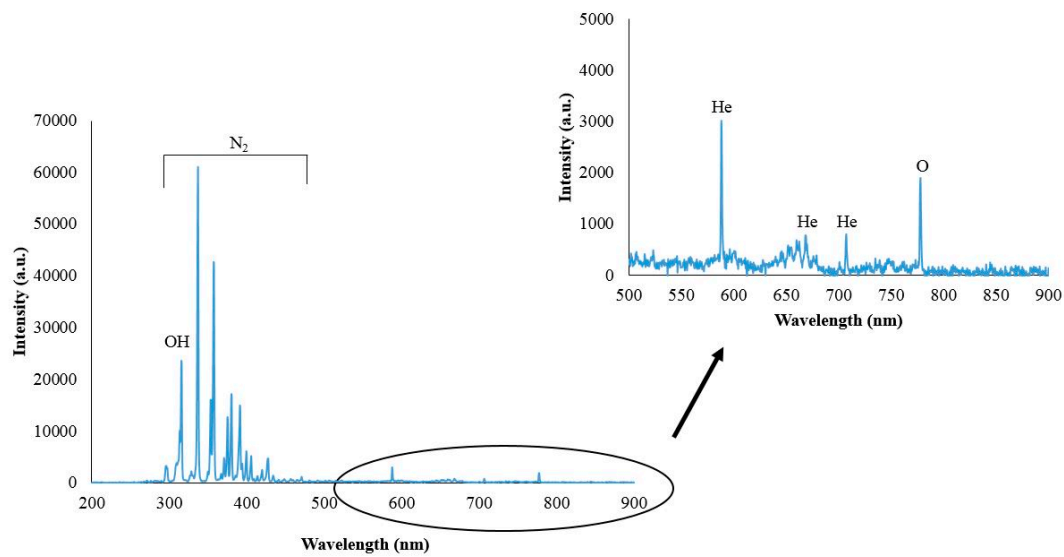
Figure 4. Typical emission spectrum of He plasma jet using 1 kHz pulse frequency and 4 μs pulse width.

2.3. Biofilm Sterilization by Combinatorial Treatment of Plasma and CHX

Biofilms were grown on titanium coupons (12.7 mm diameter and 3 mm thickness) in a CDC (Center for Disease Control and Prevention) biofilm bioreactor for 24 h in batch phase and then for 24 h under dynamic phase with agitation. Tryptic soy broth (TSB; 0.3% *w/v* for batch phase and 2% *w/v* for dynamic phase) in DI water was used for growing biofilms in the reactor at 37 °C for 48 h. An overnight culture of *Pseudomonas aeruginosa* (PAO1) was adjusted to an optical density (OD600) equivalent to 10^8 CFU/mL. The standardized bacterial suspension was used to inoculate the reactor. For the entire 48 h biofilm growth, shear stress was produced by the baffle of biofilm reactor rotating at a speed of 130 rpm to avoid the presence of planktonic bacteria. After the selected growth time, the coupons were aseptically removed from the reactor and subjected to combinatorial treatment with jet plasma and CHX (1% *v/v* in DI water). Each coupon was first plasma treated for 15, 30 and 60 s. The plasma treated coupons were then treated with CHX for 5 and 15 s. For treatment with CHX, the plasma treated coupons were submerged in CHX solution in a 24 well plate and incubated for the indicated periods of time. After treatment with CHX, the antiseptic effect was halted by adding inactivating agent solution The inactivation agent consists of a solution of Tween 80 (30 g·L^{-1}), Saponine (30 g·L^{-1}), Histidine (1 g·L^{-1}), and Cysteine (1 g·L^{-1}) [37]. After combinatorial treatment, the treated coupons were suspended in a tube with phosphate buffer saline (PBS) and sonicated for 5 min in an ultrasonic bath with vortexing for 30 s to disrupt the biofilm and release the bacterial cells. The bacterial suspension was serially diluted and plated in triplicate on TSB agar. Plates were incubated at 37 °C for 24 h and colonies were counted.

2.4. Verification of the Mathematical Model

In order to verify the mathematical model, the value of $log_{10} \frac{\phi}{\phi_0}$ for each plasma treatment time was calculated (Table 1) and these values were plotted against the CHX treatment time (Figure 5), and the diffusion lag time was then found by a linear regression according to Equation (26). The lag time was then obtained from the regression line according to the calculation of D_e from Equation (25).

Table 1. Calculated values of $log_{10}\frac{\phi}{\phi_0}$ for different chlorhexidine (CHX) treatment times after plasma treatment.

Plasma Treatment Time (s)	CHX Treatment Time (s)	$log_{10}\frac{\phi}{\phi_0}$
15	5	−0.10867783
	15	−1.29736253
30	5	−0.37619369
	15	−1.12858295
60	5	−0.01996643
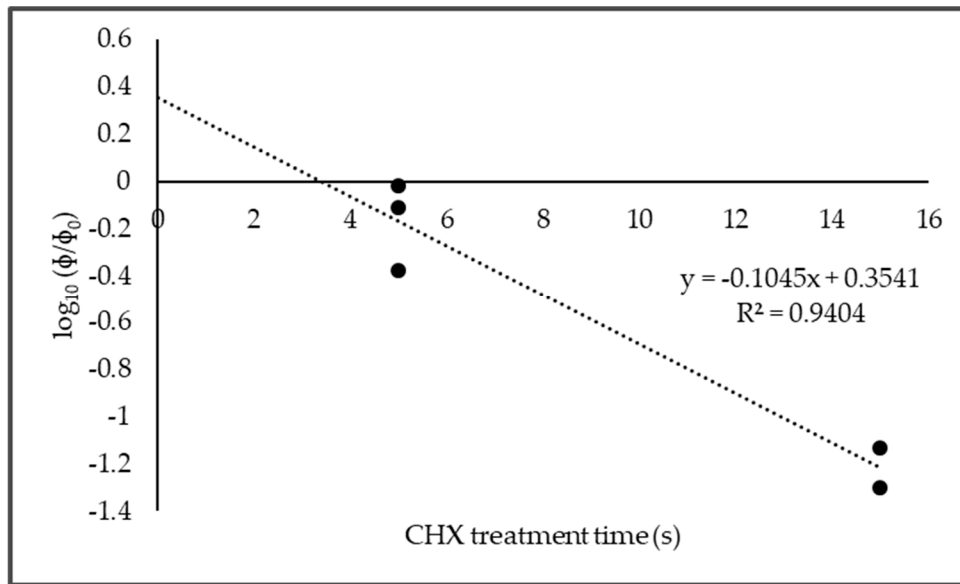
Figure 5. $Log_{10}\frac{\varnothing}{\varnothing_0}$ vs. chlorhexidine (CHX) treatment time.

From the graph in Figure 5, the x-intercept, which is t_{lag}, can be calculated as,

$$t_{lag} = \frac{0.3541}{0.1045} = 3.3 \text{ s}$$

From Equation (25), the effective diffusivity of CHX is given by the relationship $t_{lag} = \frac{32}{\pi^4}\frac{\delta^2}{D_e}$, where δ is the thickness of biofilm or 50 μm as measured by the confocal microscope (TCS SP5, Leica Microsystems). Therefore, the effective diffusivity of CHX after the plasma treatment is,

$$D_e = 2.49 \times 10^{-6} \text{ cm}^2/\text{s}$$

As we can see, this value of D_e is significantly less than the previously calculated diffusivity of CHX at 20 °C ($D_{AB} = 3.77 \times 10^{-6}$ cm^2/s), and we can conclude that the diffusion path through the biofilm is not completely open. Assuming that the tortuosity is $\sim \frac{1}{\varepsilon}$, then from Equation (5), we have,

$$\begin{aligned} \varepsilon \quad &\cong \sqrt{\frac{D_e}{D_{AB}}} \times 100\% \\ &= 81.26\% \end{aligned} \tag{27}$$

These results support our hypothesis that the plasma decontaminates the biofilm to some extent and disrupts it, which opens up the structure (~81.26% porous) to allow the CHX to get in and completely sterilize the biofilm.

We can also estimate the biofilm porosity using Maxwell's equation Fournier (4th edition), which treats the biofilm as impermeable spheres.

$$\frac{D_e}{D_{AB}} = \frac{2\varepsilon}{3 - \varepsilon} \tag{28}$$

Using the values of $D_e = 2.49 \times 10^{-6}$ cm^2/s and $D_{AB} = 3.77 \times 10^{-6}$ cm^2/s, we get $\varepsilon = 74.4\%$, which is not significantly different than the result obtained in Equation (27).

3. Conclusions

A mathematical model was developed to explain the reason behind sterilization in the combinatorial treatment order. The average porosity of the biofilm was estimated to be about 80% during the plasma treatment time, suggesting that the application of plasma is disrupting the biofilm and ultimately making it porous. This is allowing CHX to penetrate deeper inside the porous biofilm and kill all bacterial cells and sterilize the biofilm. This might be the reason behind complete sterilization in this treatment method. It should be noted, however, that more work will be needed to further validate the calculation and conclusion using various other treatment times.

References

1. Kuhn, D.; Chandra, J.; Mukherjee, P.; Ghannoum, M. Comparison of biofilms formed by Candida albicans and Candida parapsilosis on bioprosthetic surfaces. *Infect. Immun.* **2002**, *70*, 878–888. [CrossRef] [PubMed]
2. Donlan, R.M. Role of biofilms in antimicrobial resistance. *ASAIO J.* **2000**, *46*, S47–S52. [CrossRef] [PubMed]
3. Flemming, H.-C.; Wingender, J. The biofilm matrix. *Nat. Rev. Microbiol.* **2010**, *8*, 623–633. [CrossRef] [PubMed]
4. Chiba, A.; Sugimoto, S.; Sato, F.; Hori, S.; Mizunoe, Y. A refined technique for extraction of extracellular matrices from bacterial biofilms and its applicability. *Microb. Biotechnol.* **2015**, *8*, 392–403. [CrossRef] [PubMed]
5. Gupta, T.T.; Karki, S.B.; Matson, J.S.; Gehling, D.J.; Ayan, H. Sterilization of Biofilm on a Titanium Surface Using a Combination of Nonthermal Plasma and Chlorhexidine Digluconate. *BioMed Res. Int.* **2017**, *2017*. [CrossRef] [PubMed]
6. Robert, E.; Vandamme, M.; Brullé, L.; Lerondel, S.; Le Pape, A.; Sarron, V.; Riès, D.; Darny, T.; Dozias, S.; Collet, G. Perspectives of endoscopic plasma applications. *Clin. Plasma Med.* **2013**, *1*, 8–16. [CrossRef]
7. Winter, J.; Nishime, T.M.; Glitsch, S.; Lühder, H.; Weltmann, K.D. On the development of a deployable cold plasma endoscope. *Contrib. Plasma Phys.* **2018**, *58*, 404–414. [CrossRef]
8. Robert, E.; Barbosa, E.; Dozias, S.; Vandamme, M.; Cachoncinlle, C.; Viladrosa, R.; Pouvesle, J.M. Experimental study of a compact nanosecond plasma gun. *Plasma Process. Polym.* **2009**, *6*, 795–802. [CrossRef]
9. Fricke, K.; Koban, I.; Tresp, H.; Jablonowski, L.; Schröder, K.; Kramer, A.; Weltmann, K.-D.; von Woedtke, T.; Kocher, T. Atmospheric pressure plasma: A high-performance tool for the efficient removal of biofilms. *PLoS ONE* **2012**, *7*, e42539. [CrossRef] [PubMed]
10. Bourdon, A.; Darny, T.; Pechereau, F.; Pouvesle, J.-M.; Viegas, P.; Iséni, S.; Robert, E. Numerical and experimental study of the dynamics of a μs helium plasma gun discharge with various amounts of N2 admixture. *Plasma Sources Sci. Technol.* **2016**, *25*, 035002. [CrossRef]
11. Robert, E.; Darny, T.; Dozias, S.; Iseni, S.; Pouvesle, J.-M. New insights on the propagation of pulsed atmospheric plasma streams: From single jet to multi jet arrays. *Phys. Plasmas* **2015**, *22*, 122007. [CrossRef]
12. Sobota, A.; Guaitella, O.; Garcia-Caurel, E. Experimentally obtained values of electric field of an atmospheric pressure plasma jet impinging on a dielectric surface. *J. Phys. D Appl. Phys.* **2013**, *46*, 372001. [CrossRef]

13. Ayan, H.; Fridman, G.; Gutsol, A.F.; Vasilets, V.N.; Fridman, A.; Friedman, G. Nanosecond-pulsed uniform dielectric-barrier discharge. *IEEE Trans. Plasma Sci.* **2008**, *36*, 504–508. [CrossRef]

14. Vaňková, E.; Válková, M.; Kašparová, P.; Masák, J.; Scholtz, V.; Khun, J.; Julák, J. Prevention of biofilm re-development on Ti-6Al-4V alloy by cometary discharge with a metallic grid. *Contrib. Plasma Phys.* **2018**. [CrossRef]

15. Karki, S.B.; Gupta, T.T.; Yildirim-Ayan, E.; Eisenmann, K.M.; Ayan, H. Investigation of non-thermal plasma effects on lung cancer cells within 3D collagen matrices. *J. Phys. D Appl. Phys.* **2017**, *50*, 315401. [CrossRef]

16. Karki, S.B.; Yildirim-Ayan, E.; Eisenmann, K.M.; Ayan, H. Miniature dielectric barrier discharge nonthermal plasma induces apoptosis in lung cancer cells and inhibits cell migration. *BioMed Res. Int.* **2017**, *2017*. [CrossRef] [PubMed]

17. Isbary, G.; Stolz, W.; Shimizu, T.; Monetti, R.; Bunk, W.; Schmidt, H.-U.; Morfill, G.; Klämpfl, T.; Steffes, B.; Thomas, H. Cold atmospheric argon plasma treatment may accelerate wound healing in chronic wounds: Results of an open retrospective randomized controlled study in vivo. *Clin. Plasma Med.* **2013**, *1*, 25–30. [CrossRef]

18. Laroussi, M. Low temperature plasma-based sterilization: Overview and state-of-the-art. *Plasma Process. Polym.* **2005**, *2*, 391–400. [CrossRef]

19. Fridman, G.; Peddinghaus, M.; Balasubramanian, M.; Ayan, H.; Fridman, A.; Gutsol, A.; Brooks, A. Blood coagulation and living tissue sterilization by floating-electrode dielectric barrier discharge in air. *Plasma Chem. Plasma Process.* **2006**, *26*, 425–442. [CrossRef]

20. Ehlbeck, J.; Schnabel, U.; Polak, M.; Winter, J.; Von Woedtke, T.; Brandenburg, R.; Von dem Hagen, T.; Weltmann, K. Low temperature atmospheric pressure plasma sources for microbial decontamination. *J. Phys. D Appl. Phys.* **2010**, *44*, 013002. [CrossRef]

21. Scholtz, V.; Julák, J.; Kříha, V. The Microbicidal Effect of Low-Temperature Plasma Generated by Corona Discharge: Comparison of Various Microorganisms on an Agar Surface or in Aqueous Suspension. *Plasma Process. Polym.* **2010**, *7*, 237–243. [CrossRef]

22. Ehlbeck, J.; Brandenburg, R.; von Woedtke, T.; Krohmann, U.; Stieber, M.; Weltmann, K.-D. PLASMOSE-antimicrobial effects of modular atmospheric plasma sources. *GMS Krankenh. Interdiszip.* **2008**, *3*, 2–12.

23. Sato, T.; Doi, A.; Urayama, T.; Nakatani, T.; Miyahara, T. Inactivation of Escherichia coli by a coaxial microwave plasma flow. *IEEE Trans. Ind. Appl.* **2007**, *43*, 1159–1163. [CrossRef]

24. Belgacem, Z.B.; Carré, G.; Charpentier, E.; Le-Bras, F.; Maho, T.; Robert, E.; Pouvesle, J.-M.; Polidor, F.; Gangloff, S.C.; Boudifa, M. Innovative non-thermal plasma disinfection process inside sealed bags: Assessment of bactericidal and sporicidal effectiveness in regard to current sterilization norms. *PLoS ONE* **2017**, *12*, e0180183. [CrossRef] [PubMed]

25. Zelaya, A.; Vandervoort, K.; Brelles-Mariño, G. Battling bacterial biofilms with gas discharge plasma. In *Plasma for Bio-Decontamination, Medicine and Food Security*; Springer: Berlin, Germany, 2012; pp. 135–148.

26. Jiang, C.; Schaudinn, C.; Jaramillo, D.E.; Gundersen, M.A.; Costerton, J.W. A sub-microsecond pulsed plasma jet for endodontic biofilm disinfection. In *Plasma for Bio-Decontamination, Medicine and Food Security*; Springer: Berlin, Germany, 2012; pp. 179–190.

27. Machala, Z.; Tarabová, B.; Pelach, M.; Šipoldová, Z.; Hensel, K.; Janda, M.; Šikurová, L. Bio-decontamination of water and surfaces by DC discharges in atmospheric air. In *Plasma for Bio-Decontamination, Medicine and Food Security*; Springer: Berlin, Germany, 2012; pp. 31–44.

28. Sousa, J.S.; Girard, P.-M.; Sage, E.; Ravanat, J.-L.; Puech, V. DNA oxidation by reactive oxygen species produced by atmospheric pressure microplasmas. In *Plasma for Bio-Decontamination, Medicine and Food Security*; Springer: Berlin, Germany, 2012; pp. 107–119.

29. Soušková, H.; Scholtz, V.; Julák, J.; Savická, D. The fungal spores survival under the low-temperature plasma. In *Plasma for Bio-Decontamination, Medicine and Food Security*; Springer: Berlin, Germany, 2012; pp. 57–66.

30. Stewart, P.S. Theoretical aspects of antibiotic diffusion into microbial biofilms. *Antimicrob. Agents Chemother.* **1996**, *40*, 2517–2522. [PubMed]

31. Suci, P.; Mittelman, M.; Yu, F.; Geesey, G. Investigation of ciprofloxacin penetration into Pseudomonas aeruginosa biofilms. *Antimicrob. Agents Chemother.* **1994**, *38*, 2125–2133. [CrossRef] [PubMed]

32. Nichols, W.W.; Evans, M.J.; Slack, M.P.; Walmsley, H.L. The penetration of antibiotics into aggregates of mucoid and non-mucoid Pseudomonas aeruginosa. *Microbiology* **1989**, *135*, 1291–1303. [CrossRef] [PubMed]

33. Fournier, R.L. *Basic Transport Phenomena in Biomedical Engineering*, 4th ed.; CRC Press: New York, NY, USA, 2017.

34. Balagopal, S.; Arjunkumar, R. Chlorhexidine: The gold standard antiplaque agent. *J. Pharm. Sci. Res.* **2013**, *5*, 270.

35. Rasimick, B.J.; Wan, J.; Musikant, B.L.; Deutsch, A.S. Stability of doxycycline and chlorhexidine absorbed on root canal dentin. *J. Endod.* **2010**, *36*, 489–492. [CrossRef] [PubMed]

36. Gupta, T.T.; Matson, J.S.; Ayan, H. Antimicrobial Effectiveness of Regular Dielectric-Barrier Discharge (DBD) and Jet DBD on the Viability of Pseudomonas aeruginosa. *IEEE Trans. Radiat. Plasma Med Sci.* **2018**, *2*, 68–76. [CrossRef]

37. Matthes, R.; Koban, I.; Bender, C.; Masur, K.; Kindel, E.; Weltmann, K.D.; Kocher, T.; Kramer, A.; Hübner, N.O. Antimicrobial efficacy of an atmospheric pressure plasma jet against biofilms of Pseudomonas aeruginosa and Staphylococcus epidermidis. *Plasma Process. Polym.* **2013**, *10*, 161–166. [CrossRef]